Int. J.Nano Dimens. 3(1): 35-42, Summer 2012
ISSN: 2008-8868

Contents list available at **IJND**

International Journal of Nano Dimension

Journal homepage: *www.IJND.ir*

Time-dependent analysis of carrier density and potential energy in spherical centered defect InGaAs/AlGaAs quantum dot (SCDQD)

H. Hoseinkhani*
M. A. Talebian Darzi
M.Abdollahi

Department of physics, Faculty of science, I.H.U Tehran, Iran.

Received: 24 November 2011
Accepted: 02 March 2012

ABSTRACT

Interaction and correlation effects in quantum dots play a fundamental role in defining both their equilibrium and transport properties. Numerical methods are commonly employed to study such systems. In this paper we investigate the numerical calculation of quantum transport of electrons in spherical centered defect InGaAs/AlGaAs quantum dot (SCDQD). The simulation is based on the imaginary time solution of time-dependent Schrödinger equation, under effective mass approximation by using finite difference method. The self-consistent properties of the system solution of the time-dependent Schrödinger coupled with poisson equations have been self-consistently solved and the Hartree and exchange-correlation potentials as well as the penetration of wave function in the barrier regions have been calculated. Electron density and potential energy are calculated in SCDQD. The interaction between the charge carriers and corresponding barriers causes the more drastic repulsion of charge carriers from the infinite wall than the barriers within the structure. The oscillatory structures in the active region are caused by the quantum effect of tunneling and depletion near the barriers.

Keywords: *Numerical calculation; Finite difference method; Self-consistent; Quantum dot.*

INTRODUCTION

Semiconductor quantum dots are nanostructures in which the carriers are confined in all three dimensions. The difference between quantum dots and other quantum systems (quantum wires and wells) is that the energy levels in the quantum dots are completely discrete. The small size of quantum dots is an important factor that has great impact on discrete of their energy levels. These nano-particles due to their small size have unique optical and electrical properties that the electrons play a key role in appearance of these properties.

* Corresponding author:
H. Hoseinkhani
Department of physics, Faculty of Science, I.H.U Tehran, Iran.
Tel +98 9149392378
Fax +98 2177104938
Email *hhoseinkhani@yahoo.com*

Recently, quantum dots due to their wide application in laser, infrared photodetectors, quantum computing, transistors, and optical communication and many others have been recently considered. Thus, some researchers have studied their electronic structures and others the physical properties of quantum dots [1]. A considerable amount of electronic and optical work done on the quantum dot has been cited in the references [2–6]. An extensive review on electronic structure of quantum dots is reported by Reimann and Minnie [7]. Numerical simulation of transport of charge carriers in quantum dots is widely used for the analysis of physical processes in the semiconductor devices and estimation of their electrical parameters. In this research, the self-consistent properties of the system solution of the time-dependent Schrödinger coupled with poisson equations have been self-consistently solved and the Hartree and exchange-correlation potentials as well as the penetration of wave function in the barrier regions have been calculated. This paper contains the following section: The next section presents the theory and algorithm. results and discussion are given in section 3. In the last section, the conclusion has been presented.

THEORY AND ALGORITHM

To numerically calculate the properties of carriers in quantum systems, the status of wave function at each point of the mesh must be known, this requires solving the equation of motion with the initial wave function is given at each point of the mesh. Initially, the number of wave functions will be generated to fill up the Fermi level in a confined region (sphere) of radius 100nm without any barrier. This can be done by solving the time-independent or static Schrodinger Eq. 1 without any potential. The answer would be a number of standing waves corresponding to the number of states required to fill up to the Fermi level.

$$-\frac{\hbar^2}{2}\left(\frac{d}{dr}\left(\frac{1}{m(r)}\right)\frac{d}{dr}+\frac{2}{m(r)r}\frac{d}{dr}-\frac{l(l+1)}{m(r)r^2}\right)R_{i,l}(r) \quad (1)$$
$$+v(r)R_{i,l}(r)=ER_{i,l}(r)$$

In this relation, $R_{i,l}(r)$ is the radial wave function of sub band, l is the orbital quantum number, $m(r)$ is the position-dependent effective mass and $v(r)$ is the confining potential which is determined from Eq. 2.

$$v(r)=\begin{cases} o & r<R_o \\ \infty & r>R_o \end{cases} \quad (2)$$

R_o is the total radius. Using the (1) and (2) relations, wave function is obtained as follows:

$$R_{i,l}(r)=\sqrt{\frac{2}{R_0^3}}\frac{j_l(\alpha_{nl}r)}{j_{l+1}(\alpha_{nl}R_0)} \quad (3)$$

Where, j_l is the spherical Bessel function of order l and α_{nl} are the nth root of Bessel functions. So, discrete Eigen value of energy is as follows:

$$E_{nl}=\frac{\hbar^2{\alpha_{nl}}^2}{2m^*{R_0}^2} \quad (4)$$

Now, the broad band structure included the central defect in middle of quantum dot and double barrier around it are placed to form a multi-layer quantum dots (Figure 1).

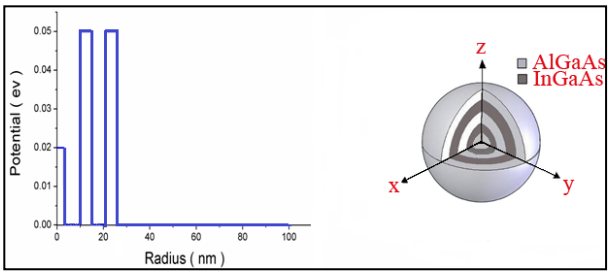

Fig. 1. Schematic and potential distribution of structure

The energy levels and charge density distribution of the system solution of the time-dependent Schrödinger coupled with poisson equations have been self-consistently solved [8].

$$HR_{i,l}(r,t) = -i\hbar\frac{\partial R_{i,l}(r,t)}{\partial t} \quad (5)$$

$$\left(\frac{d^2}{dr^2}+\frac{2}{r}\frac{d}{dr}\right)V_h(r) = -\frac{4\pi e^2}{k(r)}(n(r,t)-N_D^+) \quad (6)$$

$$H = T + V = -\frac{\hbar^2}{2}\left(\frac{d}{dr}(\frac{1}{m(r)})\frac{d}{dr}+\frac{2}{m(r)r}\frac{d}{dr}-\frac{l(l+1)}{m(r)r^2}\right) + \left[V_b(r)-eV_h(r)+V_{xc}(r)\right] \quad (7)$$

In the above relations, $V_h(r)$ is the Hartree potential, $m(r)$ is the position-dependent effective mass, $n(r,t)$ is the charge density, $k(r)$ is the dielectric constant, N_D^+ is the donor concentration, $R_{i,l}(r,t)$ is the radial wave function, $V_b(r)$ is the potential barrier, e is the electron charge, V_{xc} is the exchange-correlation potential. To obtain the actual band structure is used the finite difference method for discretization of (5) equation.

Charge density of the system, the following relation is obtained:

$$n(r,t) = \frac{1}{4\pi}\sum_{l=0}2(2l+1)\sum_{i=1}|R_{i,l}|^2 \quad (8)$$

In this equation, $\sum_{i=1}|R_{i,l}|^2$ is for any particular value of l to all bound states. $2(2l+1)$ due to the spin and magnetic quantum number has been entered.

For the Poisson equation in (6) relation, system must be in electrical equilibrium:

$$\int_0^\infty (n(r,t)-N_D^+)r^2dr = 0 \quad (9)$$

Many body effects in system with using the relation of exchange-correlation potential have been considered. The parameterized $v_{xc}(r,t)$ in units of reduced Redberg is given by [9]:

$$v_{xc}(r,t) = -\frac{1.222}{r_s(r,t)} - 0.0666\ln(1.0+\frac{11.4}{r_s(r,t)}) \quad (10)$$

Where $r_s(r,t)$ is the dimensionless radius of electrons, which is given as follows:

$$r_s(r,t) = (\frac{4\pi}{3}a^{*3}n(r,t))^{-\frac{1}{3}} \quad (11)$$

$$a^* = \frac{m_e k(r)}{m(r)}a_B$$

Where a^* is the reduced-Bohr radius, m_e is the electron mass and a_B is the Bohr radius. By solving the time-dependent Schrödinger equation in the absence of an external electric field and by substituting imaginary time $t=-it$, the ground state or equilibrium of the many electron system may be obtained. Flowchart of this process is shown in Figure 2.

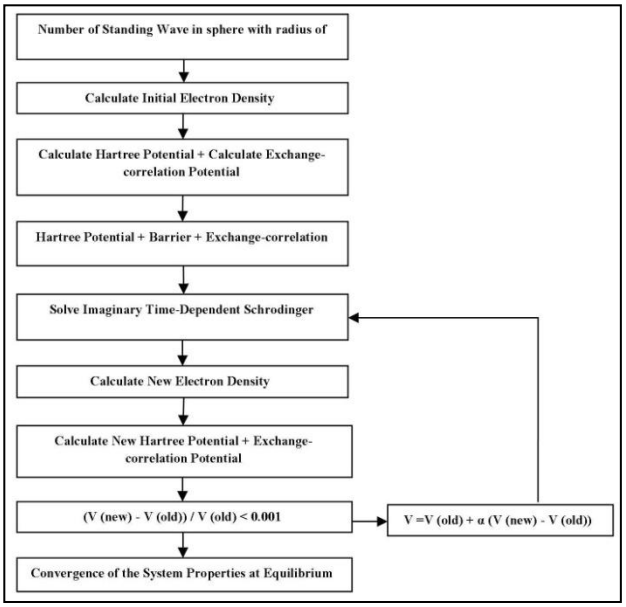

Fig. 2. The flow chart of the process of the closed system at equilibrium

RESULTS AND DISCUSSION

Properties of the system using the potential and electron density profiles at zero bias in the imaginary time evolution have been investigated. We have taken $k_{InGaAs} = 13.05$, $m_{InGaAs} = 0.064 m_e$ and $N_D^+ = 10^{17} cm^{-3}$ as material parameters. The time evolution was monitored and Figure A3-G3 and Figures A4-G4 show the progress of the observables, the potential and electron density at different moments. In Figure A3-G3 the electron density distribution profiles clearly show an immense redistribution of the carrier density at the boundaries especially near the barriers.

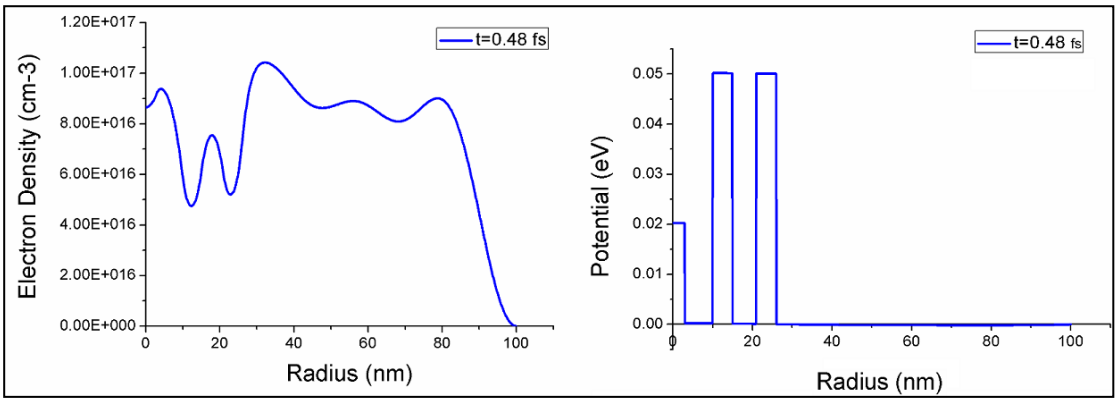

A3. Time evolution of the electron density in t=0.48 fs

A4. Time evolution of the potential in t=0.48 fs

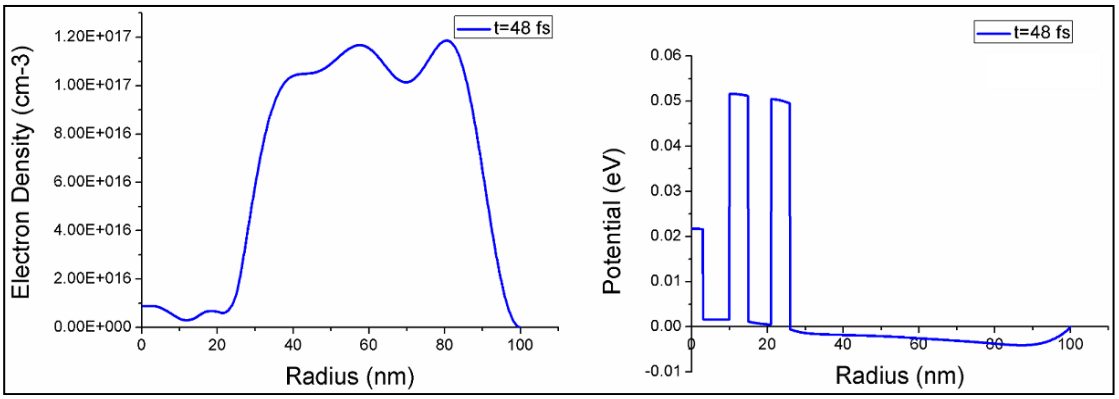

B3. Time evolution of the electron density in t=48 fs

B4. Time evolution of the potential in t=48 fs

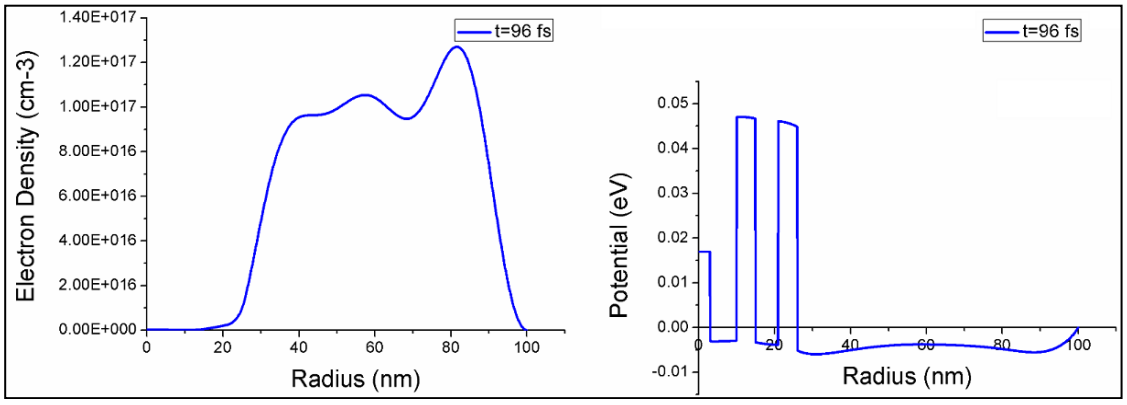

C3. Time evolution of the electron density in t=96 fs

C4. Time evolution of the potential in t=96 fs

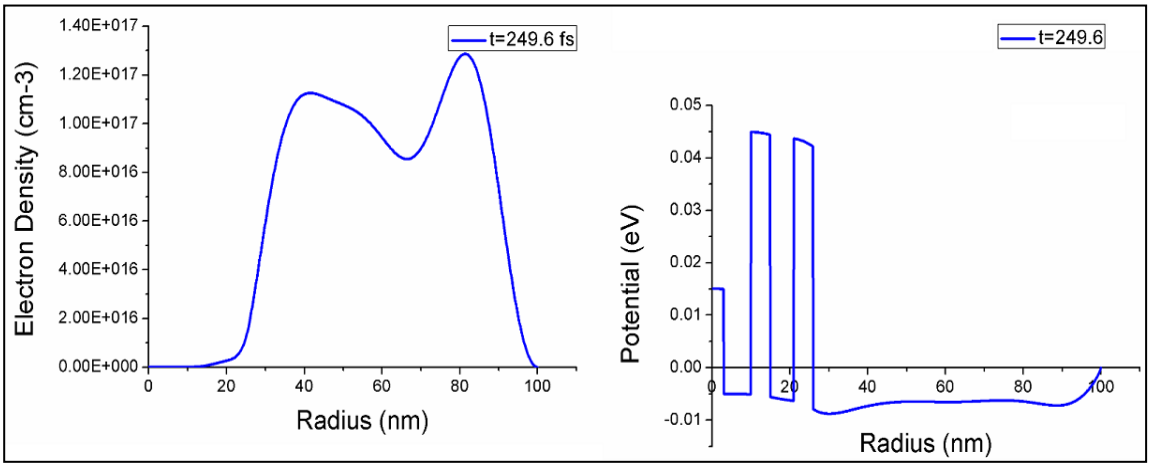

D3. Time evolution of the electron density in t=294.6 fs

D4. Time evolution of the potential in t=294.6 fs

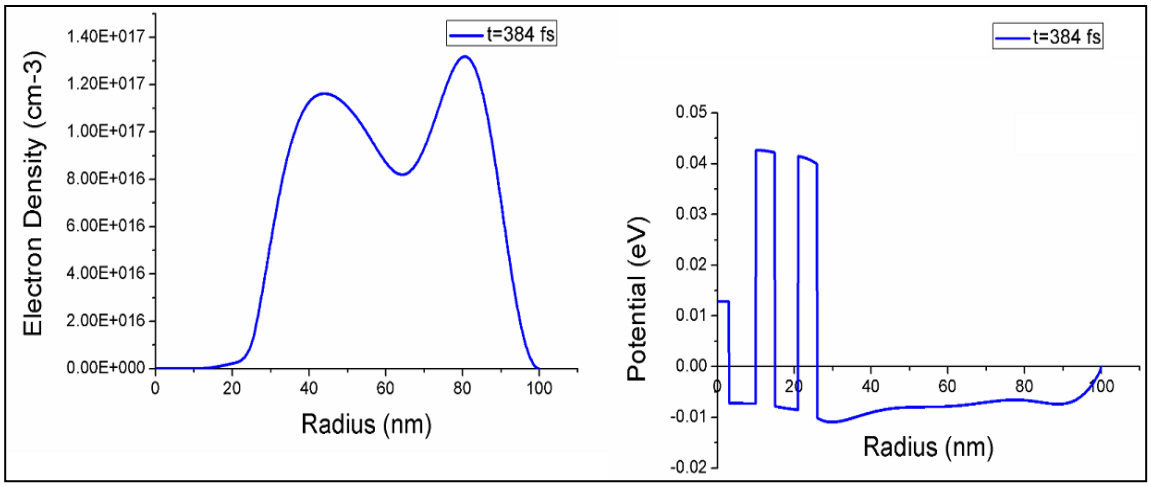

E3. Time evolution of the electron density in t=384 fs

E4. Time evolution of the potential in t=384 fs

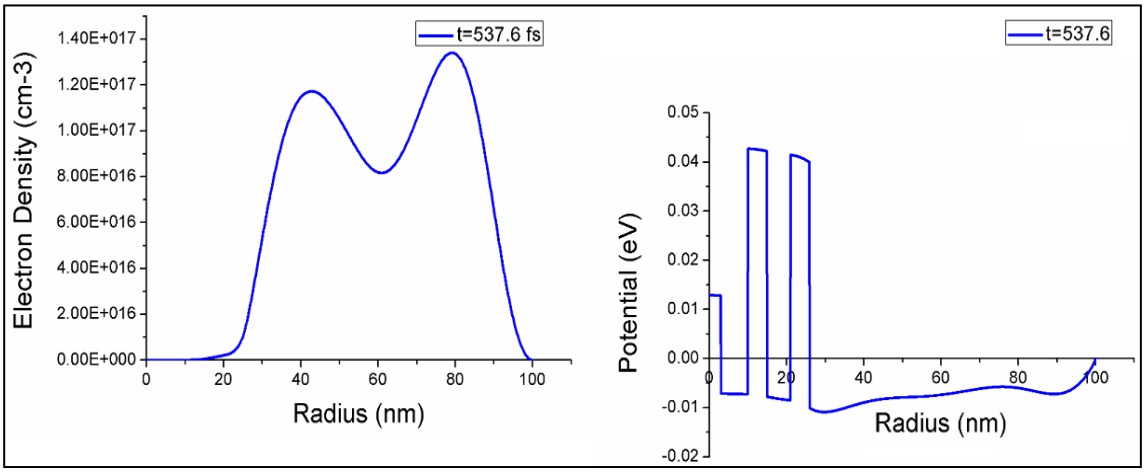

F3. Time evolution of the electron density in t=537.6 fs

F4. Time evolution of the potential in t=537.6 fs

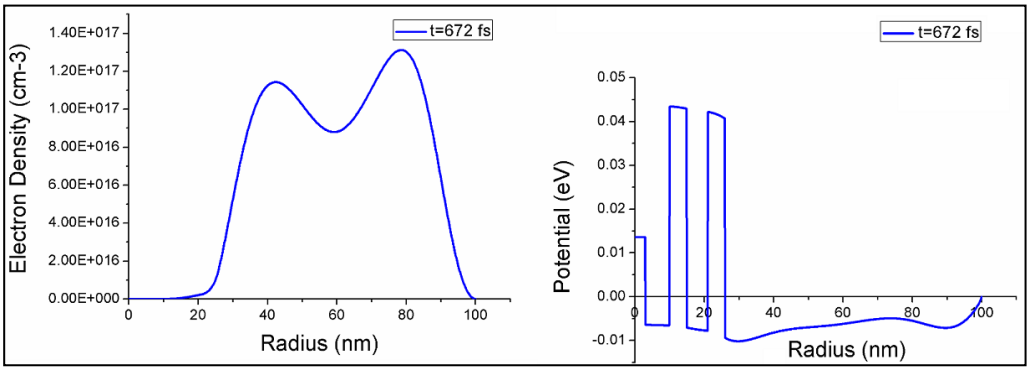

G3. Time evolution of the electron density in t=672 fs

Fig. 3. Time evolution of the electron density at different moments

G4. Time evolution of the potential in t=672 fs

Fig. 4. Time evolution of the potential at different momets

From the profiles one can see some structures being developed at the boundaries and near the barriers in the reservoirs as well. Due to the considered potential for structure the wave function outside of the sphere is zero. So that, the electron density reaches to zero at the boundary. The structures near the boundary and barriers are the result of interaction between the charge carriers and corresponding barriers. This interaction causes the more drastic repulsion of charge carriers from the infinite wall than the barriers within the structure. The structures at the boundaries are the influence of the infinite wall which is artificial and has nothing to do with the properties of the SCDQD structure. In Figure 5 the three-dimensional surface of time evolution of the electron density changes between 0.48 to 672 *fs* at zero bias, has been shown. Also, in this figure can be observed that the oscillations of electron density in primary times are more severe and after 672 *fs* reach to convergence.

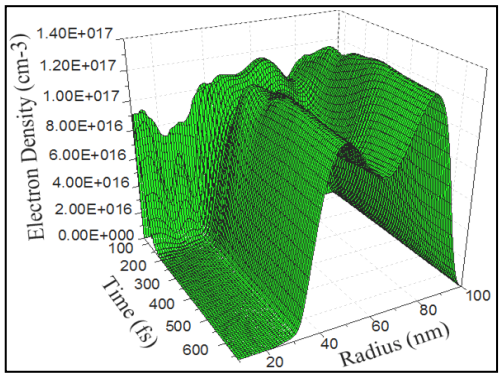

Fig. 5. 3D surface of time evolution of the electron density in a closed system

In Figure 5, changes of electron density are not visible in the active region due to a lower scale than other regions. Therefore, in Figure 6 we've drawn the electron density in logarithmic scale only for the active region. Because the barriers have a finite height and a narrow width, it becomes possible for the wave of carriers to communicate with the well through the barriers. The tiny build up in the well is the result of quantum penetration of the carriers, namely the tunnelling of the carriers into the well. In terms of quantum, the carriers are able to communicate with the well through the extension of the tails of their wave function which tunnelling through the barriers and couple with available states in the well. In general, the tunnelling problem consists of the propagation of a particle through a region where the particles energy is smaller than the potential energy. Quantum mechanically, since particles display wave features, the quantum waves can tunnel through the barrier. This is a purely quantum mechanical effect which is due to the wave aspect of microscopic objects. In the active region due to the tunnelling through the barriers and depletion at the barriers in primary times the electron density is much more and over time is reduced. Build up of carriers in the well has significant implications since it causes conduction through the device at zero bias. The tunnelling and depletion of carriers at the different regions of the system have a complementary effect which keeps the system as a whole charged neutral.

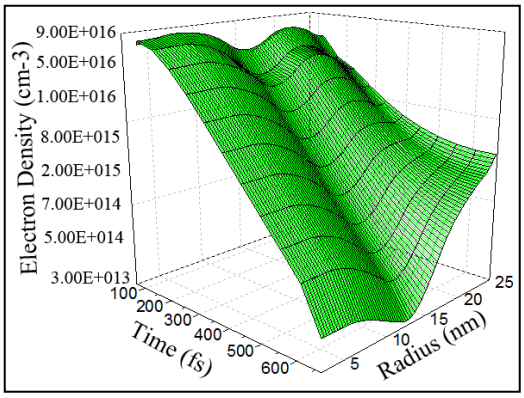

Fig. 6. 3D surface of time evolution of the electron density for active region in logarithmic scale

Similarly, in Figures A4-G4 one can see the energy band structures or potential profile has gone through a drastic change. These figures are self explanatory and their time evolution (imaginary) clearly shows that the energy band structure at the contact regions or reservoirs are symmetrically approaching a constant potential (screening contact regions). However, the profiles of data show two significant structures within each reservoir. One of them is the artificial band binding dip near the boundary which is the coupling effect of the system with infinite wall. The other is the true band bending dip near the barrier which is due to the carrier redistribution effect at the junction interface. The cause of this effect is due to the interaction of non-symmetric material properties in the junction. Also Figure 7 shows the 3D surface of time evolution of the potential profile in a closed system. The potential of system after 672 *fs* reach to convergence.

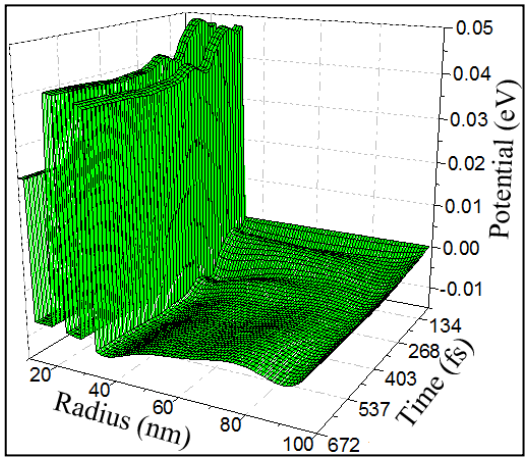

Fig. 7. 3D surface of time evolution of the potential in a closed system

CONCLUSION

For the spherical centered defect InGaAs/AlGaAs quantum dot (SCDQD), we investigated the self-consistently properties of system. At zero bias the electron density and potential after 672 *fs* reach to convergence. The oscillatory structures are caused by the quantum effect of penetration, depletion and accumulation near the barriers. The depletion and accumulation occur due to quantum repulsion at the barriers while penetration occurs due to quantum tunneling through the barriers. The depletion of carriers is a consequence of a deficit of charge carriers which extends a finite into the classically allowed region of the reservoir. An added effect of this deficit is that a small density of carriers tunneling into the classically forbidden regions of the barrier for a finite distance while the majority of the density of carriers accumulate away from the barriers in the reservoirs. Tunnelling is a purely quantum mechanical effect which is due to the wave aspect of microscopic objects.

REFERENCES

[1] G.N. Panin, T.W. Kang,T.W. Kim, S.H. Park, S.M. Si, Y.S. Ryu, H.C. Jeon, (2003), Semiconductor quantum dots created by post growth treatment. *Physica E*. 17: 484–488.

[2] L. Pichl, J. Horáček, V. Mitin, V. Ryzhiia, (2003), Tunneling effects and electron transport in quantum dot Structures. *Physica E.* 18: 83–84.

[3] T. Kwapiński, R. Taranko, (2003), Time-dependent transport through a quantum dot with the over-dot (bridge) additional tunneling channel. *Physica E.* 18: 402–411.

[4] M. Kobayashi, S. Miyahara, N. Mori, C. Hamaguchi, (2003), Electron transport in quantum dot arrays: self-consistent modeling. *Physica E.* 19: 188–191.

[5] Procolo Lucignano, Piotr Stefan´ski, Arturo Tagliacozzo, Bogdan R. Bułka, (2007), Quantum transport across multilevel quantum dot. *Current Applied Physics.* 7: 198–204.

[6] Y.X. Deng, X.H. Yan, N.S. Tang, (2009), Influences of multiterminal and time-dependent

magnetic field on the transport properties of triple quantum dots. *Physica E*. 41: 353–358.

[7] S.M. Reimann, M. Manninen, (2002), Electronic structure of quantum dots. *Rev.Mod.Phys*. 74: 1283.

[8] M. Shahi, M. Tomak, (2005), The self-consistent calculation of a spherical quantum dot: A quantum genetic algorithm study. *phisica E*. 28: 247-256.

[9] M.A. Talebian, (1998), Time-Dependent Analysis Of Transport In Resonant-Tunneling Heterostructures, Chicagoe.

Cite this article as: H. Hoseinkhani *et al.*: Time-dependent analysis of carrier density and potential energy in spherical centered defect InGaAs/AlGaAs quantum dot (SCDQD)
Int. J.Nano Dimens. 3(1): 35-42, Summer 2012